Measurement of the ^{241}Am(n,γ) cross section at the n_TOF facility at CERN

A. Oprea[1], F. Gunsing[2], P. Schillebeeckx[3], O. Aberle[4], M. Bacak[4,5,2], E. Berthoumieux[2], D. Cano-Ott[6], M. Diakaki[7,4], E. Dupont[2], B. Geslot[8], T. Glodariu[†1], J. Heyse[3], E. Mendoza[6], A. Negret[1], V. Alcayne[6], S. Amaducci[9,10], J. Andrzejewski[11], L. Audouin[12], V. Bécares[6], V. Babiano-Suarez[13], M. Barbagallo[4,14], F. Bečvář[15], G. Bellia[9,10], J. Billowes[16], D. Bosnar[17], A. Brown[18], M. Busso[19,20], M. Caamaño[21], L. Caballero-Ontanaya[13], F. Calviño[22], M. Calviani[4], A. Casanovas[22], F. Cerutti[4], Y. H. Chen[12], E. Chiaveri[4,16,23], N. Colonna[14], G. Cortés[22], M. A. Cortés-Giraldo[23], L. Cosentino[9], S. Cristallo[19,24], L. A. Damone[14,25], M. Dietz[26], C. Domingo-Pardo[13], R. Dressler[27], I. Durán[21], Z. Eleme[28], B. Fernández-Domínguez[21], A. Ferrari[4], P. Finocchiaro[9], V. Furman[29], K. Göbel[30], R. Garg[26], A. Gawlik-Ramięga[11], S. Gilardoni[4], I. F. Gonçalves[31], E. González-Romero[6], C. Guerrero[23], H. Harada[32], S. Heinitz[27], D. G. Jenkins[18], E. Jericha[5], F. Käppeler[†33], G. Kaur[2], Y. Kadi[4], A. Kimura[32], N. Kivel[27], M. Kokkoris[7], Y. Kopatch[29], M. Krtička[15], D. Kurtulgil[30], I. Ladarescu[13], C. Lederer-Woods[26], H. Leeb[5], J. Lerendegui-Marco[23], S. Lo Meo[34,35], S. J. Lonsdale[26], D. Macina[4], A. Manna[35,36], T. Martínez[6], A. Masi[4], C. Massimi[35,36], P. Mastinu[37], M. Mastromarco[4], F. Matteucci[38,39], E. A. Maugeri[27], A. Mazzone[14,40], A. Mengoni[34], V. Michalopoulou[7], P. M. Milazzo[38], F. Mingrone[4], A. Musumarra[41,10], R. Nolte[42], F. Ogállar[43], N. Patronis[28], A. Pavlik[44], J. Perkowski[11], L. Piersanti[14,19,24], I. Porras[43], J. Praena[43], J. M. Quesada[23], D. Radeck[42], D. Ramos-Doval[12], T. Rauscher[45,46], R. Reifarth[30], D. Rochman[27], C. Rubbia[4], M. Sabaté-Gilarte[4,23], A. Saxena[47], D. Schumann[27], A. G. Smith[16], N. V. Sosnin[16], A. Stamatopoulos[7], G. Tagliente[14], J. L. Tain[13], T. Talip[27], A. Tarifeño-Saldivia[22], L. Tassan-Got[4,7,12], P. Torres-Sánchez[43], A. Tsinganis[4], J. Ulrich[27], S. Urlass[4,48], S. Valenta[15], G. Vannini[35,36], V. Variale[14], P. Vaz[31], A. Ventura[35], V. Vlachoudis[4], R. Vlastou[7], A. Wallner[49], P. J. Woods[26], T. Wright[16], and P. Žugec[17](The n_TOF Collaboration)

[1]Horia Hulubei National Institute of Physics and Nuclear Engineering, Romania
[2]CEA Irfu, Université Paris-Saclay, F-91191 Gif-sur-Yvette, France
[3]European Commission, Joint Research Centre (JRC), Geel, Belgium
[4]European Organization for Nuclear Research (CERN), Switzerland
[5]TU Wien, Atominstitut, Stadionallee 2, 1020 Wien, Austria
[6]Centro de Investigaciones Energéticas Medioambientales y Tecnológicas (CIEMAT), Spain
[7]National Technical University of Athens, Greece
[8]CEA Cadarache, DES, Saint-Paul-les-Durance 13108, France
[9]INFN Laboratori Nazionali del Sud, Catania, Italy
[10]Department of Physics and Astronomy, University of Catania, Italy
[11]University of Lodz, Poland
[12]Institut de Physique Nucléaire, CNRS-IN2P3, Univ. Paris-Sud, Université Paris-Saclay, F-91406 Orsay Cedex, France
[13]Instituto de Física Corpuscular, CSIC - Universidad de Valencia, Spain
[14]Istituto Nazionale di Fisica Nucleare, Sezione di Bari, Italy
[15]Charles University, Prague, Czech Republic
[16]University of Manchester, United Kingdom
[17]Department of Physics, Faculty of Science, University of Zagreb, Zagreb, Croatia
[18]University of York, United Kingdom
[19]Istituto Nazionale di Fisica Nucleare, Sezione di Perugia, Italy
[20]Dipartimento di Fisica e Geologia, Università di Perugia, Italy
[21]University of Santiago de Compostela, Spain
[22]Universitat Politècnica de Catalunya, Spain
[23]Universidad de Sevilla, Spain
[24]Istituto Nazionale di Astrofisica - Osservatorio Astronomico di Teramo, Italy
[25]Dipartimento Interateneo di Fisica, Università degli Studi di Bari, Italy
[26]School of Physics and Astronomy, University of Edinburgh, United Kingdom
[27]Paul Scherrer Institut (PSI), Villigen, Switzerland
[28]University of Ioannina, Greece
[29]Joint Institute for Nuclear Research (JINR), Dubna, Russia
[30]Goethe University Frankfurt, Germany
[31]Instituto Superior Técnico, Lisbon, Portugal
[32]Japan Atomic Energy Agency (JAEA), Tokai-Mura, Japan
[33]Karlsruhe Institute of Technology, Campus North, IKP, 76021 Karlsruhe, Germany
[34]Agenzia nazionale per le nuove tecnologie (ENEA), Italy

[35]Istituto Nazionale di Fisica Nucleare, Sezione di Bologna, Italy
[36]Dipartimento di Fisica e Astronomia, Università di Bologna, Italy
[37]INFN Laboratori Nazionali di Legnaro, Italy
[38]Istituto Nazionale di Fisica Nucleare, Sezione di Trieste, Italy
[39]Department of Physics, University of Trieste, Italy
[40]Consiglio Nazionale delle Ricerche, Bari, Italy
[41]Istituto Nazionale di Fisica Nucleare, Sezione di Catania, Italy
[42]Physikalisch-Technische Bundesanstalt (PTB), Bundesallee 100, 38116 Braunschweig, Germany
[43]University of Granada, Spain
[44]University of Vienna, Faculty of Physics, Vienna, Austria
[45]Department of Physics, University of Basel, Switzerland
[46]Centre for Astrophysics Research, University of Hertfordshire, United Kingdom
[47]Bhabha Atomic Research Centre (BARC), India
[48]Helmholtz-Zentrum Dresden-Rossendorf, Germany
[49]Australian National University, Canberra, Australia

Abstract. The neutron capture cross section of ^{241}Am is an important quantity for nuclear energy production and fuel cycle scenarios. Several measurements have been performed in recent years with the aim to reduce existing uncertainties in evaluated data. Two previous measurements, performed at the 185 m flight-path station EAR1 of the neutron time-of-flight facility n_TOF at CERN, have permitted to substantially extend the resolved resonance region, but suffered in the near-thermal energy range from the unfavorable signal-to-background ratio resulting from the combination of the high radioactivity of ^{241}Am and the rather low thermal neutron flux. The here presented ^{241}Am(n,γ) measurement, performed with C_6D_6 liquid scintillator gamma detectors at the 20 m flight-path station EAR2 of the n_TOF facility, took advantage of the much higher neutron flux. The current status of the analysis of the data, focussed on the low-energy region, will be described here.

1 Introduction

The cross section of the ^{241}Am(n,γ) reaction is an important quantity for a number of nuclear technology applications. In recent years several efforts on evalutions and measurements have been undertaken worldwide to improve the knowledge of the ^{241}Am(n,γ) cross section, in particular in the thermal and epithermal energy region. The ^{241}Am(n,γ) cross section is listed in the NEA High Priority Request List [1, 2]. Work by the WPEC subgroup 41 [3] and a critical review of measured thermal cross sections [4] are examples of evaluations. As for time-of-flight measurements, previously two capture experiments, one with C_6D_6 detectors [5] and one with BaF_2 [6], have been performed at the long 185 m flight path EAR1 of the n_TOF facility. For both experiments the same sample was used. Those measurements have substantially increased the resolved energy region to 320 eV while evaluations previously went only up to 150 eV. The thermal neutron flux at this long flight path is rather low because of the use of borated water, strongly suppressing the gamma-ray background from neutron capture in hydrogen, but at the same time removing slow neutrons from the beam by capture in boron.

The two capture measurements [5, 6] suffer from a large systematic uncertainty at low neutron energy caused by the large background component due to the radioactivity of ^{241}Am, in spite of the use of a 2 mm lead screen. The gamma-ray background at thermal energies was about 90% of the signal. After corrections, both measurements were found to be inconsistent at low neutron energies. To resolve this discrepancy, a new capture measurement with C_6D_6 detectors was performed using the same sample, but now at the new 20 m vertical flight path EAR2. Because of the shorter flight path, the thermal flux per unit of time of flight is about a factor 10 higher. In addition, the neutrons in the vertical direction are moderated by normal water, resulting in a supplementary factor of about 40 for the thermal flux relative to the long flight path [7]. The 20 m flight path EAR2 therefore seems to be well adapted for capture measurements in the thermal and epithermal region, where the focus of the present experiment lies. Time-of-flight measurements covering the full thermal region are a welcome complement to integral techniques typically used at reactors in this energy region. Note that the spallation target in use for this experiment was still the second generation target and not the recent upgraded target [8] with optimized performances. Special care has to be taken to extract the correct resolution function from the simulated data [9].

2 Experimental setup and preliminary spectra

The present experiment measuring data to extract the ^{241}Am(n,γ) cross section in the thermal region and the first few resonances at low energy has been carried out at the EAR2 station of the n_TOF facility at CERN [10]. Three neutron-insensitive C_6D_6 liquid scintillator detectors have been used to measure gamma rays following neutron capture as a function of the neutron time of flight. Proton pulses with a nominal intensity of 7×10^{12} protons per pulse at a minimum repetition rate of 1.2 s generated neutron by hitting the 40 cm thick and 60 cm diameter cylindrical lead target. The water cooling circuit served as a moderator resulting in a neutron beam with energies from thermal up to a few GeV.

The sample with a mass of 32.23 ± 0.19 mg of Am and an activity of 4.1 GBq, the same as used in the previous

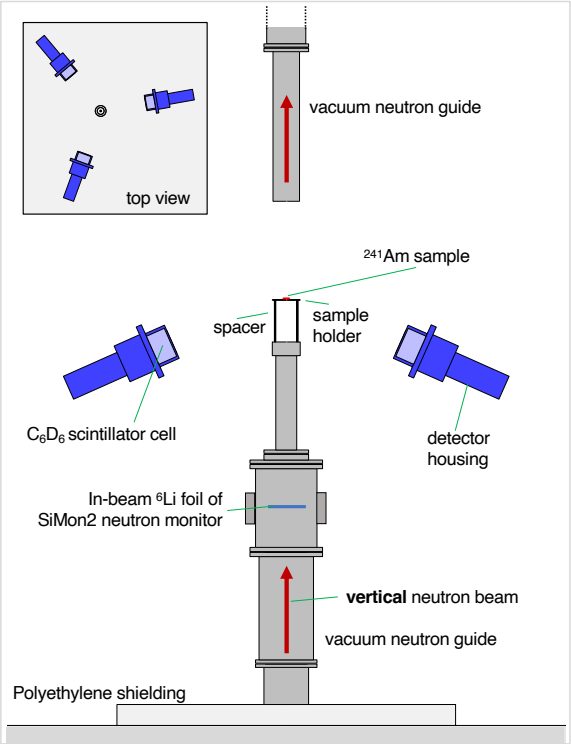

Figure 1. A schematic view of the detectors and sample setup used for the present experiment. The inset with the top view shows the three detectors used. The detectors were held in place using carbon fibre rods which are not shown in the figure.

experiments, consists of americium oxide ($^{241}AmO_2$), infiltrated and immobilized in a pressed pellet of aluminum oxide (Al_2O_3) forming a rigid disk of 12.26 mm diameter, encapsulated in a sealed aluminum container. A second, similar sample with a mass of 40.98 ± 0.25 mg was also used, as well as a dummy sample consisting of a similar aluminum oxide pellet but without americium, used for background measurements. In addition to those samples we also measured several other samples in the same configuration inside an identical aluminum container, among which ^{197}Au and ^{103}Rh for the absolute normalization using their low-energy saturated resonances.

The distance from the sample to the detectors of about 40 cm was chosen such that the high radioactivity did not notably impact the bias current of the photomultipliers. We could therefore avoid the need for a lead shielding which allowed for the use a lower gamma-ray threshold in the data analysis, in particular the pulse height weighting function as used with the total energy method.

The setup of the three detectors including the sample inside a sample holder were modelled in GEANT4 in order to simulate the gamma-ray response to mono-energetic gamma-rays. Those responses are needed to calculate the pulse height weighting function, which makes the detector efficiency of the gamma-ray cascade independent of the gamma-ray energy [11, 12]. The setup is shown in figure 1.

Upstream of the sample, the SiMon2 detector [13], consisting of a thin in-beam ^{6}Li foil and four off-beam sil-

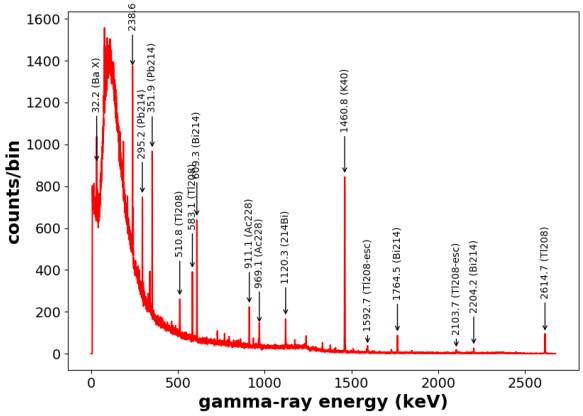

Figure 2. The natural background in the experimental area EAR2, as measured with a HPGe detector. The presence of ^{40}K and the decay series of ^{232}Th and ^{238}U is clearly visible.

icon detectors, was installed to measure the neutron flux at the same time. This detector was also an important ingredient of the evaluated neutron flux typically used for experiments [7].

The used data acquisition system was based on Teledyne SP Devices digitizers, sampling the detector waveforms with steps of 1 ns and a resolution of 12 bits for a time window of 100 ms after each TOF pulse. The waveforms, after zero suppression, were transferred to CERN's long-term storage facility for off-line event building. Detector events, consisting of the time of flight and the pulse height extracted from the waveforms, were constructed for each detector and used for further analysis.

Energy calibrations of the C_6D_6 detectors were done without beam using standard gamma-ray sources ^{137}Cs, ^{88}Y, ^{60}Co and a mixed Am-Be source. The spectra from the sources showed gain shifts over time during the measurement period. We therefore used a continuous calibration on a run-by-run basis using either the radioactivity of

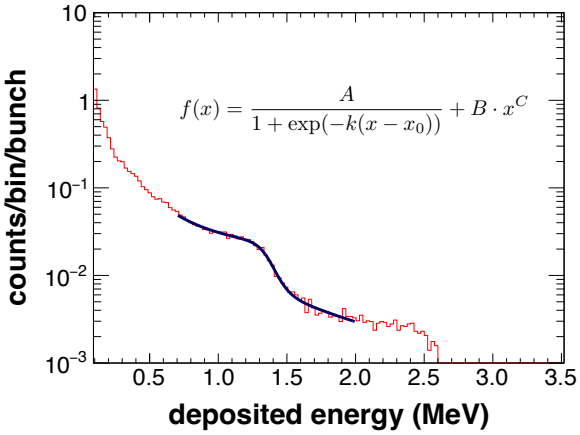

Figure 3. The measured energy deposit spectrum in the C_6D_6 detectors for times of flight larger than 50 ms. The spectrum reveals the Compton edge of the ^{40}K peak. The position fitted with a sigmoid based on the logistic function serves as energy calibration.

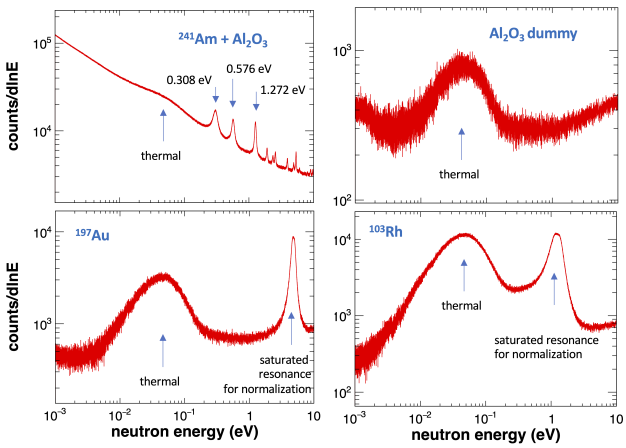

Figure 4. Comparison of raw counting spectra for the ^{241}Am sample, the dummy sample, and for ^{197}Au and ^{103}Rh. In the last two samples a saturated resonance, used for normalization is visible. The high thermal neutron flux is also well visible in all spectra.

the ^{241}Am sample, or the response to the ambient background, in particular the 1.460 MeV gamma ray from ^{40}K, present in the concrete of the walls of the experimental area. The radioactive background from the ^{241}Am sample mainly originates from the strong 59.5 keV gamma ray of ^{237}Np following the α-decay of ^{241}Am. Smaller background gamma rays come from α-induced reactions, mainly on ^{27}Al present in the aluminum oxide sample pellet.

The ambient background spectrum shown in figure 2 was measured with a high purity germanium detector and clearly shows a typical natural background including the ^{40}K peak and other smaller peaks due to the ^{232}Th and ^{238}U decay series. This response, since it is rather weak, becomes only visible when the neutrons from the beam are practically absent. This occurs at very long times of flight corresponding to an equivalent neutron energy below 1 meV given the energy distribution of the neutron beam. We used the last 50 ms of the recorded part of each time-of-flight cycle to obtain the spectrum measured by the C_6D_6 detectors in which the Compton edge of the ^{40}K peak is fairly visible. We fitted the shape of the spectra with a logistic-based sigmoid function on top of a smooth background for each run with nonradioactive samples. From the fitted sigmoid parameters we deduced the channel-energy calibration factor of the deposited energy spectra. An example of such a pulse height spectrum measured with the C_6D_6 detectors and the fit in the vicinity of the Compton edge is shown in figure 3.

In figure 4 we show the low-energy raw counting spectra for the ^{241}Am sample, together with a spectrum of the dummy sample and that of a ^{197}Au and ^{103}Rh sample. The spectra are measured as time of flight and here represented as a function of approximate energy. The Au and Rh spectra each show a saturated resonance which serves as normalization of the capture yield. In all four spectra the shape of the thermal peak is clearly visible.

3 Conclusion

The here presented experiment shows the capability of n_TOF EAR2 to peform neutron capture measurements in the low energy range, covering at the same time both the full thermal region and resonances. The measured nucleus ^{241}Am has a very high radioactivity hindering neutron capture time-of-flight measurements. In the described setup we used the high instantaneous flux of the EAR2 station of the n_TOF facility for a favorable signal to noise ratio, in combination with an increased distance between detector and sample to overcome the strong influence of the radioactivity on the photomultiplier bias. In this way there was no need for additional detector shielding and the total energy method could be employed with a low gamma-ray threshold. Gain shift issues were eventually solved by a run-by-run calibration using ^{40}K present in the natural background. A full re-analysis of the data with this much improved energy calibration is currently ongoing.

References

[1] https://www.oecd-nea.org/dbdata/hprl/
[2] E. Dupont et al., EPJ Web of Conferences **239**, 15005 (2020)
[3] *Improving nuclear data accuracy of the Am-241 capture cross-section* (2020), NEA/NSC/R(2020)2, `https://www.oecd-nea.org/download/wpec/documents/volume41.pdf`
[4] G. Žerovnik, P. Schillebeeckx et al., Nucl. Instr. Meth. A **877**, 300 (2018)
[5] K. Fraval et al., Phys. Rev. C **89** (2014)
[6] E. Mendoza et al., Phys. Rev. C **97** (2018)
[7] M. Sabaté-Gilarte et al., Eur. Phys. J. A **53** (2017)
[8] R. Esposito et al., Phys. Rev. Acc. Beams **24** (2021)
[9] V. Vlachoudis et al., *On the resolution function of the n_TOF facility: a comprehensive study and user guide* (2021), nTOF-PUB-2021-001; CERN-nTOF-PUB-2021-001
[10] A. Mengoni et al. (2022), *these proceedings*
[11] U. Abbondanno et al., Nucl. Instr. Meth. A **521**, 454 (2004)
[12] A. Borella et al., Nucl. Instr. Meth. A **577**, 626 (2007)
[13] L. Cosentino et al., Rev. Sci. Instr. **86**, 073509 (2015)